Available online at www.sciencedirect.com
ScienceDirect
International Journal of Heat and Mass Transfer 51 (2008) 1061–1070
International Journal of HEAT and MASS TRANSFER
www.elsevier.com/locate/ijhmt

Dropwise condensation heat transfer on ion implanted aluminum surfaces

M.H. Rausch, A.P. Fröba *, A. Leipertz

Lehrstuhl für Technische Thermodynamik (LTT), Universität Erlangen-Nürnberg, Am Weichselgarten 8, D-91058 Erlangen, Germany

Received 3 January 2007
Available online 10 July 2007

Abstract

Stable dropwise condensation (DWC) of saturated steam has been achieved on an aluminum alloy Al 6951 disc with an average surface finish of about 0.15 μm by means of ion beam implantation technology with an ion dose of 10^{16} N^+ cm^{-2} and an implantation energy of 20 keV. Measurements of the condensation heat transfer coefficient at steam pressures of 1200 and 1400 mbar were carried out as a function of surface subcooling on vertical plates of the same material which is commonly used for heat transfer equipment. Probably due to alloy inhomogeneities, only on about 50% of the plate surface DWC could be achieved, resulting in a maximum enhancement factor of 2.0 for DWC in comparison with theoretical values calculated by a corrected form of the Nusselt film theory. The heat transfer coefficient increases with increasing steam pressure and decreases with increasing surface subcooling. Furthermore, it was shown that condensation heat transfer cannot be enhanced if the ion implantation does not induce DWC. For the investigations, two different condensers have been used, one for the stability tests on discs and one for the heat transfer measurements on plates.

Keywords: Dropwise condensation; Heat transfer coefficient; Ion implantation; Aluminum alloys; Contact angle

1. Introduction

Condensation heat transfer is an interesting issue for technical applications as large amounts of heat can be transferred isothermally when the vaporization enthalpy is set free during transition from the vapor to the liquid phase. The appearing condensation form is directly connected with the wettability of the surface, which is predominantly determined by the surface energies of both solid and condensate as well as by the solid's surface roughness. Most condenser surfaces are made of metals which possess high surface free energies (0.5–5 N m^{-1}) and thus exhibit filmwise condensation (FWC) due to their very good wettability for all working fluids of technical interest. On the other hand, it is well known since the works of Schmidt et al. [1] in 1930 that the condensation heat transfer coefficient can be enhanced by up to one order of magnitude by adjusting dropwise condensation (DWC), allowing, e.g., a size reduction of industrial condensers. This cannot only result in decreasing space requirements and investment costs, but also operation costs can be reduced because of the lower pumping power required for the cooling fluid. Since the discovery of the advantages of DWC, many efforts have been made to induce this condensation form on metallic surfaces, but up to now none of the investigated methods could be established in real technical applications because in most cases long-term stability over several years cannot be obtained. For producing DWC on metals, a reduction of their free surface energy is necessary which could either be obtained by applying hydrophobic layers of organic substances [2–5], inorganic compounds [6], polymers [7,8] or hard coatings [9–12] to the surface or by the formation of surface alloys [13,14]. Unfortunately, most of these methods suffered from mechanical instability and thus could not be introduced to standard condensers yet.

* Corresponding author. Tel.: +49 9131 85 29789; fax: +49 9131 85 29901.
E-mail address: apf@ltt.uni-erlangen.de (A.P. Fröba).

0017-9310/$ - see front matter © 2007 Elsevier Ltd. All rights reserved.
doi:10.1016/j.ijheatmasstransfer.2006.05.047

Nomenclature

A	area (m^2)
c	specific heat capacity ($J\,kg^{-1}\,K^{-1}$)
g	acceleration of gravity ($m\,s^{-2}$)
h	heat transfer coefficient ($W\,m^{-2}\,K^{-1}$)
Δh	specific heat of vaporization ($J\,kg^{-1}$)
k	thermal conductivity ($W\,m^{-1}\,K^{-1}$)
$\dot{m}$	mass flow ($kg\,s^{-1}$)
$\dot{q}$	heat flux density ($W\,m^{-2}$)
R_a	average surface finish (m)
r	surface area factor in Wenzel's relation (–)
s	distance (m)
T	temperature (K)
x	plate height (m)

Greek symbols

Δ	difference (–)
Θ	contact angle (rad)
ρ	density ($kg\,m^{-3}$)
μ	dynamic viscosity (Pa s)
σ	interfacial tension ($N\,m^{-1}$)

Subscripts

ad	advancing
c	condensate, condensation
cw	cooling water
eq	thermodynamic equilibrium
in	inlet conditions
LV	liquid to vapor interface
l	local value
m	mean value
Nu	Nusselt film theory
out	outlet conditions
p	constant pressure
pl	plate
R	with consideration of surface roughness
re	receding
SL	solid to liquid interface
SV	solid to vapor interface
s	steam
surf	surface
1	position 1
2	position 2

Abbreviations

DWC	dropwise condensation
FWC	filmwise condensation

Surface modifications using ion implantation were introduced by Zhao et al. [15–18] as an additional technique for achieving DWC on metals, however, a quite complicated method of preparation and implantation was used which is not easily applicable in industrial scales. In the research group at the LTT Erlangen, the application of the ion implantation technique for the generation of DWC on metallic surfaces was optimized and simplified during the past decade with the goal of establishing this method as a standard technique for achieving DWC. So far, stable DWC could be obtained on stainless steel and chromed copper. Heat transfer measurements with saturated steam showed that a significant enhancement of the condensation heat transfer coefficient in comparison to FWC can be achieved on vertical surfaces, single tubes, and tube bundles [19–21].

Due to their relatively low specific weight and large thermal conductivity, aluminum alloys are commonly used materials for heat transfer components in aeronautical engineering. As weight reduction is a very important task in this field in order to optimize operation costs caused by fuel consumption, the application of DWC in the condenser of the air conditioning system of planes is of great interest. Up to now, there is only one work in which DWC could be achieved on the alloy AlCuMgPb F38, but after only five weeks the condensation form turned to FWC, probably due to oxidation effects [20].

The aim of this work is the achievement of DWC on the aluminum alloys Al 3003 and Al 6951 which are commonly used in the construction of heat transfer components in aeronautical engineering. The first part of the work was carried out using aluminum alloy discs. With a systematic variation of the implantation method and the ion implantation parameters, e.g., ion dose, and implantation energy, DWC could be induced on Al 6951. In contrast to this, on Al 3003 only a mixture of FWC and DWC was achieved. For the successful combination of material and ion implantation parameters, heat transfer measurements were carried out on vertical plates within the second part of this work.

2. Wettability and DWC

The condensation form generated on a surface generally depends on the wettability of the solid surface with the working fluid used. Wettability can be understood as the formation of phase boundaries between solid, liquid, and vapor, and it is determined by the interactions of these phases. It can be described by the contact angle in thermodynamic equilibrium Θ_{eq} which can be found between the solid surface and the tangent on the droplet surface crossing the contact line of all three phases as shown in Fig. 1. The size of the contact angle is determined by a balance of forces which is given for smooth surfaces neglecting the acceleration of gravity by Young's law [22]:

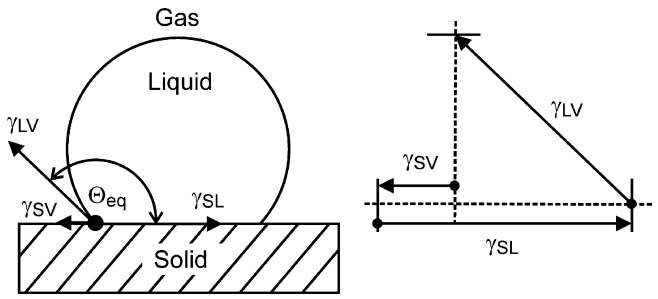

Fig. 1. Equilibrium contact angle and interfacial tension vector diagram for a single droplet for incomplete surface wettability.

$$\cos\Theta_{eq} = \frac{\sigma_{SV} - \sigma_{SL}}{\sigma_{LV}}, \tag{1}$$

where σ_{SV}, σ_{SL}, and σ_{LV} are the interfacial tensions between solid and vapor, solid and liquid, and liquid and vapor, respectively.

For the contact angle, the interfacial tension between solid and vapor σ_{SV} is decisive and in the case of metals delivers small contact angles describing excellent wettability. In order to achieve DWC, large equilibrium contact angles are required. A minimum value of 60° is given by Straub and Waas [23], and 90° should be reached in order to get optimum DWC with a small droplet departure diameter [24]. Ion implantation is able to reduce the surface energy of metals and thus the interfacial tension between the metal surface and the vapor phase of the working fluid. The method is explained in detail elsewhere [21].

When the solid surface is rough, Eq. (1) has to be modified, resulting in

$$\cos\Theta_{eq,r} = r\frac{\sigma_{SV} - \sigma_{SL}}{\sigma_{LV}} = r\cos\Theta_{eq}, \tag{2}$$

which is known as Wenzel's relation [25] and where r is the actual area of a rough surface related to its projected area. On rough surfaces, $r > 1$ always holds, which results in increased contact angles $\Theta_{eq,r}$ on rough surfaces if $\Theta_{eq} > 90°$ is valid on the plain surface and vice versa. From this point of view, it can be followed that for DWC, a certain roughness of the condensation surface is desirable if the contact angle on the smooth surface is larger than 90°, while the surface should be as plain as possible in case that

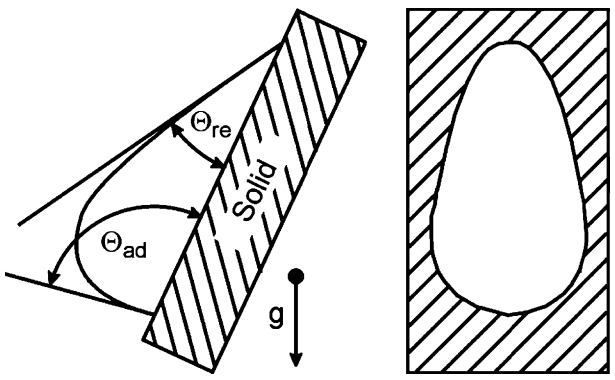

Fig. 2. Droplet behavior on inclined surfaces forming the two contact angles Θ_{re} and Θ_{ad}.

$\Theta_{eq} < 90°$. This requisite for smaller contact angles can also be derived from the phenomenon of contact angle hysteresis, which is defined as the difference of the advancing and receding contact angles Θ_{ad} and Θ_{re}, respectively, of a droplet moving on an inclined surface, see Fig. 2 [26]. For DWC, a small contact angle hysteresis is advantageous, which can be achieved by a small surface roughness [27]. Large contact angle hysteresis results in low receding contact angles which can lead to the formation of streaks behind moving droplets and finally, a condensate film spreading on the surface.

3. Experimental

The aluminum alloy samples have been prepared and treated by ion implantation with a wide range of implantation parameters. The samples were tested concerning the appearing condensation form in a condenser constructed for visual observation and stability tests. Afterwards, the heat transfer characteristics of selected samples were investigated in another condenser equipped for high accuracy heat transfer measurements. In this apparatus, a comparison of the heat transfer performance between implanted or unimplanted samples showing FWC and implanted samples showing DWC was carried out. In both condensers, deionized water was used as working fluid, and all investigations were carried out under saturation conditions.

3.1. Surface preparation

The main alloy components of the investigated aluminum alloys Al 3003 and Al 6951 are listed in Table 1 [28]. For the visual observation, discs with a diameter of 60 mm and a thickness of 12 mm were prepared, while for the heat transfer measurements, plates with a condensation area of 240 mm × 50 mm and a thickness of 10 mm were used. In order to investigate the effect of surface roughness, for each combination of ion implantation parameters one sample with $R_a \approx 0.5$ μm and one polished sample with $R_a \approx 0.15$ μm was prepared. Three different ion implantation techniques were used. Two of them are ion beam methods, what means that an ionized gas is accelerated and bundled to an ion beam which scans over the sample surface, see e.g., Ref. [29]. The difference between the two ion beam methods is that in one case, all ions produced are used for implantation, while in the other case the ion beam is separated by magnetic fields generating several beams, each containing only one kind of ion with its specific weight and charge [29]. The third method used is plasma ion implantation, where a plasma of cations is produced and the sample is charged negatively so that the ion cloud is accelerated to the sample [29]. This technique is particularly advantageous for the homogeneous implantation of non-planar geometries like tubes as reported in Ref. [21].

For all implantations, nitrogen ions were selected due to the results obtained with stainless steel and chromed copper as base materials in previous works [20,21]. In the case

Table 1
Alloy composition of the aluminum alloys Al 3003 and Al 6951 [28]

Alloy	Al (%)	Cu (%)	Fe (%)	Mn (%)	Si (%)	Zn (%)	Others (%)
Al 3003	96.7–99	0.05–0.2	<0.7	1.0–1.5	<0.6	<0.1	<0.15
Al 6951	<97	0.15–0.4	<0.8	0.4–0.8	0.2–0.5	<0.2	<0.15

of the selective ion beam implantation, N^+ was chosen. The ion dose was varied between 10^{15} and $10^{17}\,cm^{-2}$. The applied implantation energies, which directly affect the implantation depth depending on the base material qualities, ranged from 5 to 40 keV.

3.2. Apparatus for visual observation and stability tests

The appearing condensation form on the sample discs and the stability of DWC with saturated steam at atmospheric pressure were investigated in the apparatus schematically shown in Fig. 3. It is similar to the apparatus described in Ref. [20] and consists of two identical condensers (a), in each of which five samples can be tested simultaneously. In both condensers, a closed cycle of evaporation and condensation is established, and the operating pressure is given via the steam temperature control (b). Two electrical heaters (c) keep the water in the bottom of the condenser boiling, while the saturated steam is condensed on the sample surfaces (d). The condensate runs down the condenser walls back to the water pool where it is re-evaporated. In order to achieve condensation, the samples have to be cooled. For this they are directly connected to finned channels (e), through which ambient air is blown by fans (f). The condensation can be observed through heated windows in the condenser walls (g). The apparatus can be operated continuously for several months for testing the stability of DWC.

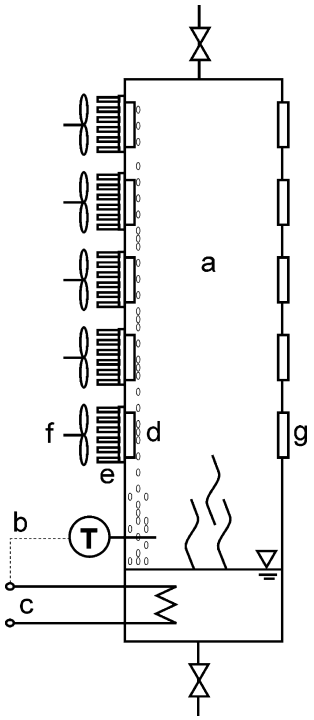

Fig. 3. Experimental condenser for visual observations and stability tests: (a) condenser; (b) temperature control system; (c) heating elements; (d) condensation surface; (e) finned air channels; (f) fans; (g) heated windows.

3.3. Apparatus for heat transfer measurements on vertical plates

The condensation heat transfer coefficient and the heat flux can be determined in another experimental condenser designed for saturated steam at steam pressures ranging from 1000 to 1500 mbar, see Fig. 4. The steam is produced in an evaporator (1) heated by four heating elements (2), each of them with a maximum heating power of 9 kW and connected to a thyristor plate (3) which ensures the control of the steam pressure inside the evaporator. Fresh water is fed into the evaporation chamber from a water tank (4) by a supply pump (5). The steam pressure in the condenser is manually adjusted by a pressure reduction valve (6) and measured with a calibrated pressure transducer with an uncertainty of ±5 mbar. The absence of non-condensable gases is ensured by a venting valve (7) close to the vertical condensation surface. The sample plates (8) are cooled on the backside by an upward directed cooling water stream. The cooling water is circulated in a closed system (9) by a cooling water pump (10). Its volume flow can be adjusted by two manual valves and is measured using a magnetic-inductive volume flow meter with an uncertainty of ±0.5%. The condensation heat is transferred from the primary system to an external cooling water system via a plate heat exchanger (11). The condensate is taken out of the condenser using a steam trap (12) and cooled by a condensate cooler (13). The condensate mass flow is determined by weighting the condensate mass leaving the condenser within a certain time period. The condensate produced on the condenser walls is collected separately (14) and does not affect the condensate mass flow measurement. The temperatures of the steam, the condensate, and the cooling water in front of and behind the sample plate are measured with resistance probes Pt100-Ω. The surface temperature of the sample, which is needed for the calculation of the heat transfer coefficient, can be determined by the application of the one-dimensional Fourier's law, which is valid in the vertical center line of the plate, see Fig. 5. This procedure for the determination of the surface temperature has already been applied successfully in the apparatus described by Koch et al. [11]. Three couples of resistance probes Pt100-Ω with a diameter of 0.7 mm are inserted into holes eroded with high precision into the

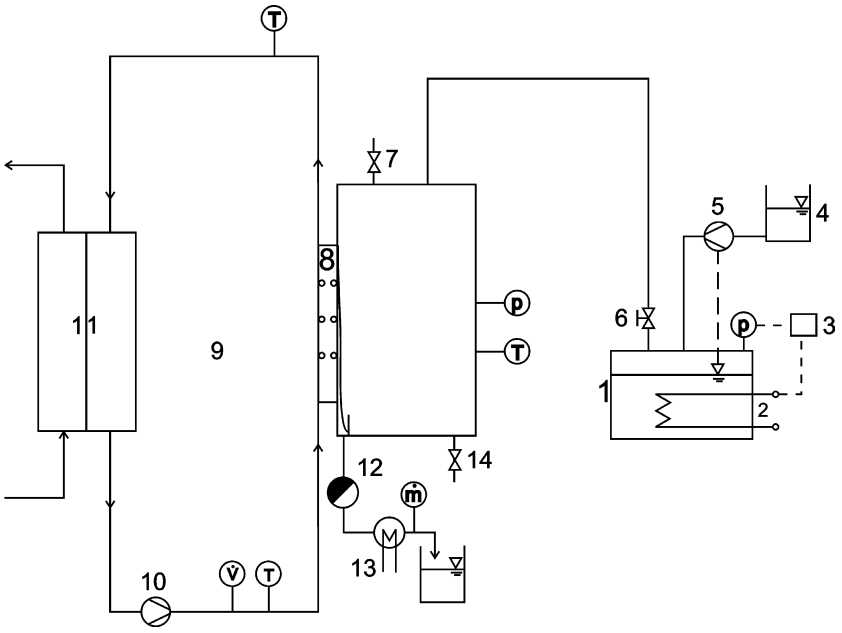

Fig. 4. Experimental apparatus for heat transfer measurements on vertical plates: (1) evaporator; (2) heating elements; (3) thyristor plate; (4) water tank; (5) supply pump; (6) pressure reduction valve; (7) venting valve; (8) sample plate; (9) cooling water cycle; (10) cooling water pump; (11) plate heat exchanger; (12) steam trap; (13) condensate cooler; (14) wall condensate departure.

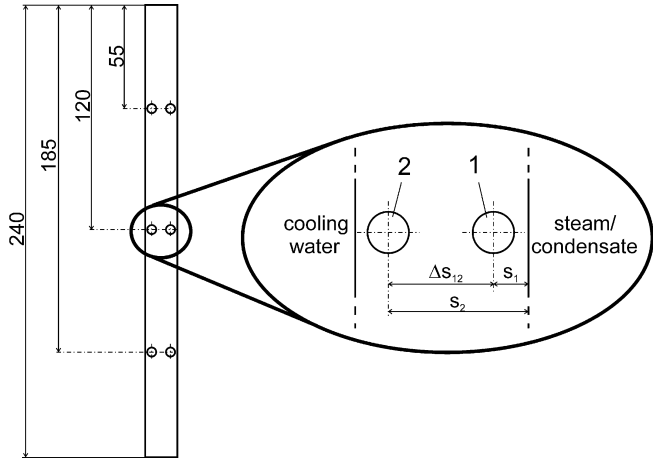

Fig. 5. Measurement of the temperature gradient inside the sample plate.

plates in order to measure the temperature gradient inside the plate. By this an extrapolation to the local plate surface temperature at three points is possible. The average of the three calculated surface temperatures is used for the determination of the condensation heat transfer coefficient. All resistance probes are calibrated with an absolute uncertainty of ±0.02 K.

During the measurements, the instability was observed to be ±0.01 g s^{-1} for the condensate mass flow due to evaporation effects and ±0.2 l min^{-1} for the cooling water flow caused by small pressure and flow fluctuations in the cooling water cycle. The maximum temperature instabilities observed were ±0.3 K for the temperatures of the steam, the condensate and the cooling water inlet and outlet due to both steam and cooling water flow fluctuations, and ±5.0 K and ±0.4 K for the temperatures inside the sample plate for DWC and FWC, respectively. The large instability of the plate temperatures for DWC is caused by the dynamics of this condensation mode. When big droplets are present on the part of the condensation surface which affects the temperature measurement, they provide a larger heat transfer resistance than small droplets and thus the surface temperature is reduced. When these big droplets depart due to their size or are washed off by other droplets running down from the top of the plate, free surface and small new droplets at the relevant area with a lower heat transfer resistance enable a rise in the surface temperature. In order to obtain a proper mean surface temperature, an average over about 90 single measurements within 30 min was taken for the calculation of the surface temperature used for the determination of the surface subcooling. For every set of experimental conditions, the standard deviation for the measured temperatures inside the sample plate was calculated and used as input for error estimations. Maximum standard deviations of 2.7 K and 0.4 K were found for DWC and FWC, respectively.

4. Data evaluation

The heat flux transferred in the experimental apparatus can be calculated in three different ways, see also Ref. [11]. The heat flux density on the condensate side $\dot{q}_c$ can be determined by

$$\dot{q}_c = \dot{m}_c[\Delta h + c_{p,c}(T_s - T_c)]A^{-1}, \quad (3)$$

where $\dot{m}_c$ is the condensate mass flow, Δh is the evaporation enthalpy, $c_{p,c}$ is the isobaric heat capacity of the conden-

sate, T_s and T_c are the temperatures of the steam and the condensate, respectively, and A is the heat transfer area. The heat flux density on the cooling water side $\dot{q}_{cw}$ can be calculated by

$$\dot{q}_{cw} = \dot{m}_{cw} c_{p,cw} (T_{cw,out} - T_{cw,in}) A^{-1}, \quad (4)$$

where $\dot{m}_{cw}$ is the cooling water mass flow, $c_{p,cw}$ is the isobaric heat capacity of the cooling water, and $T_{cw,out}$ and $T_{cw,in}$ are the temperatures at the cooling water outlet and inlet, respectively. A third possibility is the determination of the local heat flux densities inside the sample plate $\dot{q}_{pl,l}$ via Fourier's law

$$\dot{q}_{pl,l} = \frac{k_{pl}}{\Delta s_{12}} (T_1 - T_2), \quad (5)$$

where k_{pl} is the thermal conductivity of the plate, Δs_{12} is the distance between the resistance probes, and T_1 and T_2 are the temperatures measured with these at positions 1 and 2, respectively. The mean value of the three measurement points of the local temperature gradient in the sample plate results in a mean heat flux density $\dot{q}_{pl,m}$ for the whole plate used for further calculations.

In the experiments, all three possibilities for the determination of the heat flux density were carried out, and for small surface subcoolings, they sometimes differed more than 30%. Error estimation for all three methods was done for every single measurement. The errors of $\dot{q}_{cw}$ and $\dot{q}_{pl,l}$ increase with decreasing cooling water flow rate because of the decreasing temperature differences between cooling water inlet and outlet and between inner and outer measurement point in the plate, respectively. In all cases the heat flux density calculation on the condensation side $\dot{q}_c$ showed by far the smallest errors, not exceeding 1.8%. Due to this result, $\dot{q}_c$ was used for the following calculations.

Local surface temperatures $T_{surf,l}$ of the sample plate can be determined by an extrapolation of the temperatures measured inside the plate to the plate surface:

$$T_{surf,l} = T_1 + \frac{\dot{q}_{pl,l}}{k_{pl}} s_1 = T_1 + \frac{T_1 - T_2}{\Delta s_{12}} s_1 \quad (6)$$

with the assumption of the validity of Fourier's law in its one-dimensional form, which is justified in the vertical center of the plate. Here, s_1 stands for the distance between the eroded hole closer to the steam chamber and the plate surface. Again, the mean value of the three local measurement points results in a mean surface temperature $T_{surf,m}$ used for the evaluation of the mean heat transfer coefficient on the condensate side

$$h_c = \frac{\dot{q}_c}{(T_s - T_{surf,m})}, \quad (7)$$

where $(T_s - T_{surf,m})$ is the so-called mean subcooling of the condenser surface. Using the local heat flux densities $\dot{q}_{pl,l}$ and the local surface temperatures $T_{surf,l}$, three local heat transfer coefficients along the vertical axis of the condenser plate can be calculated as well. For the mean heat transfer coefficients on the condensate side, errors between 1.7% for FWC at large subcoolings and 19.0% for DWC at small subcoolings were found.

The results for the measured mean heat transfer coefficients h_c are compared with those values calculated by the corrected form of Nusselt film theory:

$$h_{Nu} = 1.15 \left[0.0206 \left(\frac{\Delta h \cdot \mu_c}{k_c \cdot (T_s - T_{surf,m})} \right)^{1/2} + 0.79 \right] \times 0.943 \left[\frac{\rho_c \cdot \Delta\rho \cdot g \cdot \Delta h \cdot k_c^3}{\mu_c \cdot (T_s - T_{surf,m}) \cdot x} \right]^{1/4}, \quad (8)$$

where ρ_c is the condensate density, $\Delta\rho$ is the difference between the densities of condensate and steam, g is the acceleration of gravity, k_c is the thermal conductivity of the condensate, μ_c is the dynamic viscosity of the condensate, and x is the height of the plate. The last part of Eq. (8) represents the original Nusselt film theory [30], which in our case has to be corrected due to several reasons. As wave formation was observed on the condensate film during the FWC experiments, the heat transfer enhancement due to this phenomenon has to be taken into account which can be adequately done by the correction factor 1.15 [31]. Inertia effects, which are neglected in Nusselt's considerations, can be included by the empirically obtained second term in Eq. (8) [32]. The variation of the physical properties of the condensate with temperature has also to be considered. Here, the viscosity shows the dominant effect which can be compensated by calculating all physical properties of the condensate at the mean temperature:

$$T_m = 0.75 \cdot T_{surf,m} + 0.25 \cdot T_s, \quad (9)$$

while only Δh and the density of the saturated steam are calculated at T_s [33]. During the measurements, Reynolds numbers for the condensate film between 35 and 120 were found. As the critical value for water of about 200 was not reached, film turbulence can be neglected [34].

5. Results and discussion

5.1. Visual observation and stability of the condensation form

Extensive experimental work has been carried out in order to adjust DWC on the aluminum alloys Al 3003 and Al 6951 with an average surface finish of both $R_a \approx 0.15$ μm and 0.5 μm. In the past, very good results with stainless steel as base material were achieved using an ion dose of 10^{16} cm^{-2} and an implantation energy of 20 keV [20,21]. Calculations with the simulation software SRIM [35] showed that in aluminum alloys, implantation energies of about 4–8 keV should lead to similar penetration depths of the doting elements as in stainless steel in the former experiments with 20 keV. With this knowledge, the first series of samples were implanted using ion beam implantation technology with a nitrogen ion dose of 10^{16} cm^{-2} and implantation energies of 5, 10, and 20 keV. Installed into the test rig for visual observation, all samples showed either perfect FWC or a stationary

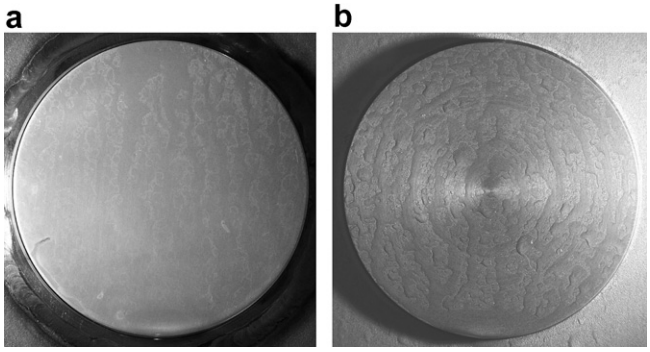

Fig. 6. FWC on polished Al 3003 (a) and stationary drops and streaks on unpolished Al 6951 (b), both treated with ion beam implantation technology with a nitrogen ion dose of 10^{16} cm^{-2} and an implantation energy of 10 keV.

image of streaks and droplets without any dynamics, which can be regarded as non-ideal FWC. In comparison with unimplanted samples, no differences could be found. The polished discs were mostly covered with a closed condensate film shown in Fig. 6a by an Al 3003 disc implanted with 10 keV, while on the unpolished samples, represented by an Al 6951 disc also implanted with 10 keV in Fig. 6b, the stationary mixture of streaks and droplets predominated. Obviously, smooth surfaces tend to produce closed condensate films so that it becomes clear that the surface roughness has a strong effect on the quality of FWC. In Fig. 6a, it can also be seen that the oxidation process of the alloy surface is not homogeneous, which leads to non-uniform colors and is probably caused by a certain inhomogeneity of the alloy material itself.

Further investigations have been executed with another series of sample discs treated with plasma ion implantation using nitrogen ion doses of 10^{15}, 10^{16}, and 10^{17} cm^{-2}, and implantation energies of 10, 20, and 40 keV. In this case, the samples were partially shielded during the ion implantation process leading to a partially ion implanted surface so that condensation on implanted and unimplanted surfaces could be observed directly next to each other. Again, the two kinds of condensation described above appeared on all samples on both the implanted and unimplanted areas so that no effect of the surface modification compared to the untreated surfaces could be found.

In a third set of experiments, polished and unpolished samples of both aluminum alloys were partially treated with ion selective ion beam implantation technology. N^+ ions, which showed the best results in earlier investigations with stainless steel and chromed copper [20], were implanted with an ion dose of 10^{16} cm^{-2} and an implantation energy of 20 keV. Lower energies could not be applied due to the characteristics of the implantation equipment. As shown in Fig. 7, on both unpolished Al samples (Fig. 7a and b) perfect FWC appeared. On the polished Al 3003 sample shown in Fig. 7c, a mixed form of FWC and DWC was formed. The DWC zones were located on the upper and the left border of the implanted part of the

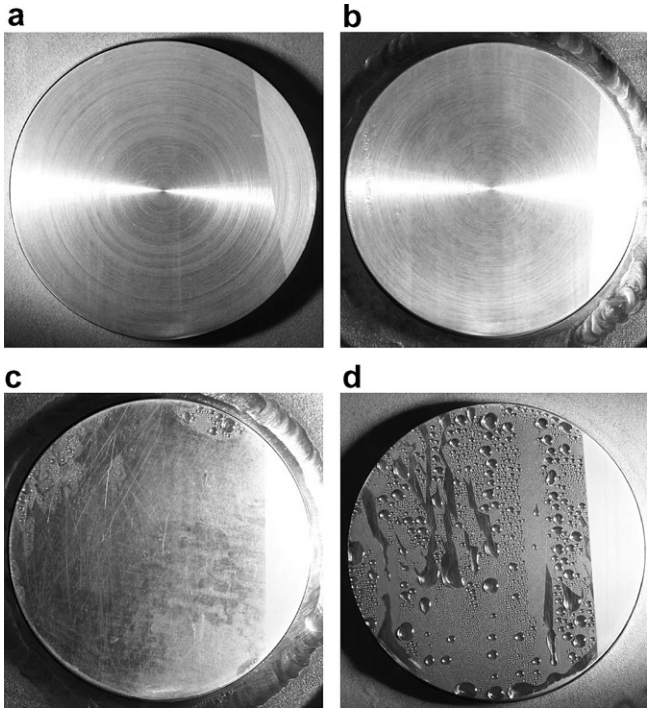

Fig. 7. FWC on unpolished Al 3003 (a) and on unpolished Al 6951 (b), mixed FWC/DWC on the implanted part of polished Al 3003 (c) and DWC on the implanted part of polished Al 6951 (d); all samples treated with ion selective ion beam implantation technology with an ion dose of 10^{16} N^+ cm^{-2} at an implantation energy of 20 keV.

disc. The light zones on the right hand side of the samples were the unimplanted areas on which a different oxidation behavior took place than on the implanted areas. From this observation it can be followed that the surface modification obviously has an effect on the oxidation process, which only slightly affected the condensation form in the cases discussed up to now. In Fig. 7d, it can be seen that on the implanted part of the polished Al 6951 sample, DWC could be adjusted, while on the unimplanted area, a closed condensate film was formed. Inside the DWC zone, small permanent streaks were observed. These streaks did not change with time and thus can be considered to be formed on alloy inhomogeneities. Here, the applied ion implantation could not produce a surface modification suitable for the adjustment of DWC. Comparing the four samples shown in Fig. 7, it becomes clear that the implementation of DWC on aluminum alloys is a very sensitive task. On the one hand, the ion implantation for two different alloys with a polished surface only lead to pure DWC on Al 6951 although the two materials hardly differ in their alloy composition and characteristics. On the other hand, the surface roughness also seems to have a decisive effect as on the polished Al 6951 sample DWC could be obtained while on the unpolished ideal FWC was formed.

The reproducibility could be proved with another Al 6951 disc on which four different surfaces were produced. Again, the polished implanted area showed DWC while on the unpolished implanted and both unimplanted areas

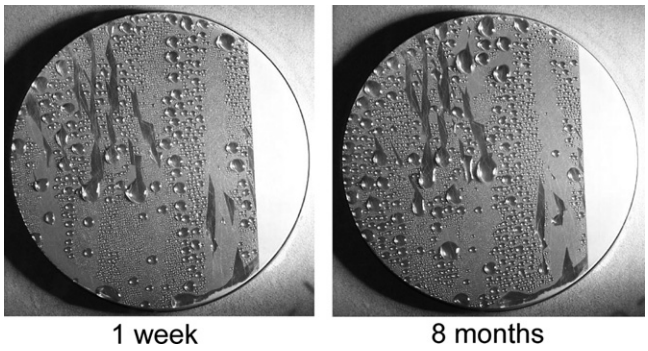

Fig. 8. Time behavior of DWC on polished Al 6951 treated with ion selective ion beam implantation technology with an ion dose of 10^{16} N^+ cm^{-2} at an implantation energy of 20 keV.

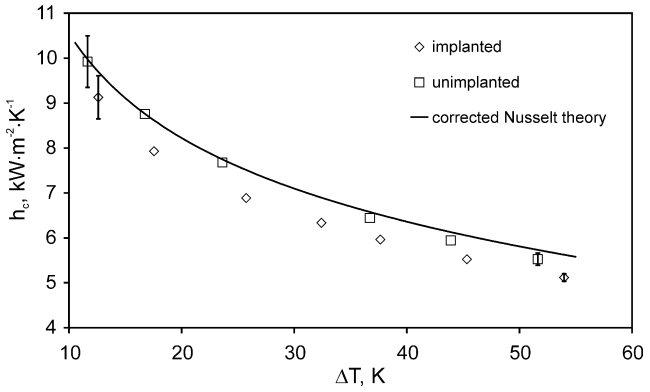

Fig. 9. Experimental values of the heat transfer coefficient h_c for FWC on unimplanted and implanted unpolished Al 6951 plates at a steam pressure of 1400 mbar in comparison with theoretically calculated values for FWC as a function of surface subcooling.

FWC was formed. Stability of DWC on the polished Al 6951 sample could be shown for 8 months, which can be seen in Fig. 8. During this time, condensation of saturated steam was constantly maintained. Afterwards, the sample was exposed to ambient air for 2 months and then reinstalled into the condenser. At the beginning, DWC appeared on the implanted part of the disc, but within only a few hours the mirror-like polished surface was covered with an oxide layer and the condensation form turned to FWC. Obviously in ambient air a thin oxide layer was formed and grew further in contact with saturated steam, leading to FWC.

As a result of the extensive work done concerning the adjustment of DWC on aluminum alloys, it can be stated that the selective ion beam implantation of N^+ ions with an ion dose of 10^{16} cm^{-2} and an implantation energy of 20 keV in Al 6951 with an average surface finish of approximately $R_a \approx 0.15$ μm is able to implement stable DWC, which, in spite of the observed oxidation effects, is a very promising result for the future use of the benefits of this condensation form in technical applications.

5.2. Heat transfer measurements

The heat transfer coefficient was measured as a function of the surface subcooling at different steam pressures for polished and unpolished and both unimplanted and implanted Al 6951 sample plates. The ion implantation parameters were chosen as found to promote DWC during the visual observation.

The results obtained for the two unpolished samples were compared to each other and to theoretical values calculated by Eq. (8). With the investigation of these samples, the possibility of heat transfer enhancement also in the FWC regime using ion implantation technology was checked. It is well known that ion implantation is able to reduce the surface energy of metallic surfaces [15], which results in a reduction of the wettability with the condensate and thus decreases the adhesion forces between metal and fluid. Consequently, enhanced condensate flow may be possible leading to smaller film thickness, which is the dominating heat transfer resistance in FWC. As a result, ion implantation technology may be able to enhance condensation heat transfer without even inducing DWC.

As expected from the qualitative results gained on the previously tested sample discs, both unpolished plates showed perfect FWC for all steam pressures and cooling water flow rates. The measurement results at a steam pressure of 1400 mbar presented in Fig. 9 show that the above mentioned possible effect obviously did not occur. On the implanted sample the measured h_c values were even smaller than on the implanted one due to unknown surface effects produced by ion implantation. Measurements at a steam pressure of 1200 mbar showed identical results. For the Al samples under investigation, ion implantation technology is only able to enhance condensation heat transfer if DWC can be achieved. In addition, the measured values confirmed the operational reliability of the measurement equipment and the cleanliness of the apparatus. The values calculated from the corrected Nusselt film theory were in good agreement with the experiment. The maximum errors in h_c for all FWC experiments were between 1.7% and 7.2%, and the largest errors were found for the smallest subcooling.

In further heat transfer measurements, the unimplanted and implanted polished Al 6951 samples were investigated. On the unimplanted sample shown in Fig. 10a, FWC was formed, while on about 50% of the surface area of the implanted sample, DWC was achieved as can be seen in Fig. 10b. This phenomenon is probably caused by the inhomogeneity of the aluminum alloy so that on some parts of the surface the implantation could not fulfill its task and no DWC could be achieved due to the fluctuation in the material characteristics over the surface. This observation is in accordance with the results of the visual observation on sample discs.

As can be seen in Fig. 11, the h_c values measured for the unimplanted plate showing FWC correspond well with the theoretical values for both investigated steam pressures. The theoretical values shown in Fig. 11 were calculated

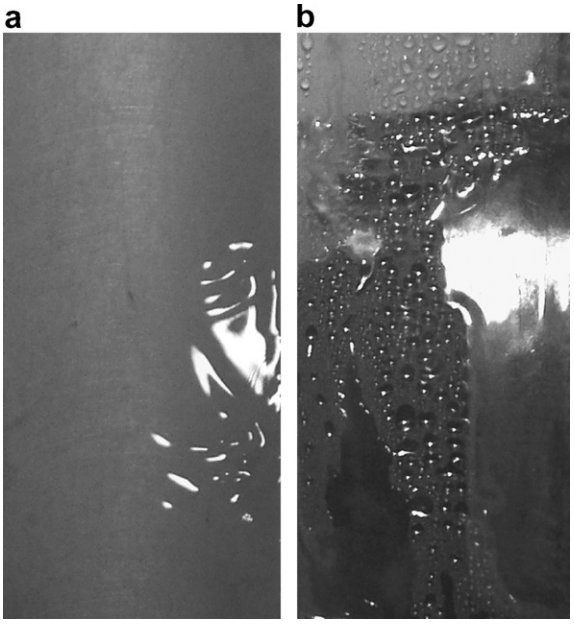

Fig. 10. FWC on unimplanted (a) and mixed DWC and FWC on implanted (b) polished Al 6951 plates.

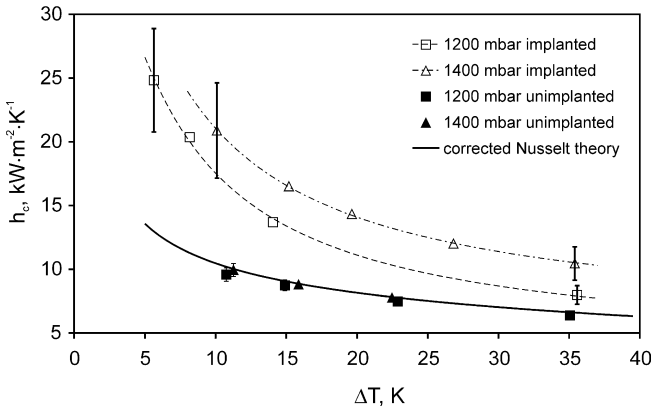

Fig. 11. Experimental values of the heat transfer coefficient h_c on unimplanted and implanted polished Al 6951 plates showing FWC and partial DWC, respectively, at different steam pressures in comparison with theoretically calculated values for FWC as a function of surface subcooling.

for 1200 mbar and are almost identical for 1400 mbar. For FWC, the error bars at higher subcoolings are within the symbols. The adjustment of DWC on the implanted plate leads to a distinct increase in the heat transfer coefficient compared to FWC. The largest values for h_c could be achieved at the smallest surface subcooling. This effect was caused by the decrease of condensate mass present on the condensation surface with decreasing subcooling, so that the heat transfer resistance through the water on the surface was also reduced. In addition, higher steam pressures also increased the heat transfer coefficient by reducing the mass transfer resistance between steam and condensate [36]. At a steam pressure of 1400 mbar and $\Delta T = 10.1$ K, h_c could be enhanced by a factor of 2.0 relative to the corrected Nusselt film theory, while at a steam pressure of 1200 mbar and $\Delta T = 5.6$ K, a maximum enhancement factor of 1.9 was reached. For smaller ΔT, which could not be reached due to limitations of the used cooling system, even larger h_c values can be expected. Maximum errors of $\pm 12\%$ and $\pm 18\%$ for h_c at 1400 mbar were found for $\Delta T = 35.5$ K and 10.1 K, respectively. In the case of 1200 mbar, the maximum errors decreased to $\pm 9\%$ and $\pm 19\%$ at $\Delta T = 35.6$ K and 8.2 K, respectively. In comparison to former results on implanted stainless steel plates, where an enhancement factor of about 4.0 was observed, the smaller factor for implanted Al 6951 is caused by the film zones on the plates, which locally increase the heat transfer resistance.

6. Conclusions

DWC of saturated steam near atmospheric pressure was obtained on polished Al 6951 with an average surface finish of $R_a \approx 0.15$ μm applying ion selective ion beam implantation with an ion dose of 10^{16} N^+ cm^{-2} and an implantation energy of 20 keV. The reproducibility and stability of the achieved condensation form have been proved for 8 months. It was found that aluminum alloys are very sensitive to the implantation parameters. A small change in the alloy composition results in a change of the implantation parameters in order to achieve DWC. The surface roughness also has a decisive effect on the obtained condensation form. For aluminum alloys, smooth surfaces seem to be preferred for the adjustment of DWC.

Measurements of the condensation heat transfer coefficient as a function of the surface subcooling showed that FWC heat transfer on Al 6951 cannot be enhanced by ion implantation. In contrast, DWC on about 50% of the condensation surface causes an enhancement of the heat transfer coefficient. In this work, a maximum enhancement factor of 2.0 in comparison with the corrected Nusselt film theory was found. Further enhancement is expected for surfaces completely covered with DWC and for smaller subcoolings. The DWC heat transfer coefficient increases with decreasing subcooling and with increasing steam pressure.

The successful adjustment of DWC on the aluminum alloy Al 6951 used in aeronautical engineering and the observed enhancement of condensation heat transfer is a decisive step in opening new possibilities in the optimization of heat transfer systems for aircraft.

Acknowledgements

The authors gratefully acknowledge the financial support of parts of the work by the Federal Ministry of Economics and Labor (BMWA, Bundesministerium für Wirtschaft und Arbeit) in form of the joint research project EOSYS (FKZ 20K0301H) and of parts by the German National Science Foundation (DFG).

References

[1] E. Schmidt, W. Schurig, W. Sellschopp, Versuche über die Kondensation von Wasserdampf in Film- und Tropfenform, Tech. Mech. Thermodyn. 1 (2) (1930) 53–63.

[2] L.C.F. Blackman, M.J.S. Dewar, H. Hampson, An investigation of compounds promoting the dropwise condensation of steam, Appl. Chem. 7 (1957) 160–171.

[3] A.K. Das, H.P. Kilty, P.J. Marto, G.B. Andeen, A. Kumar, The use of an organic self-assembled monolayer coating to promote dropwise condensation of steam on horizontal tubes, J. Heat Transfer 122 (2000) 278–286.

[4] S. Vemuri, K.J. Kim, An experimental and theoretical study on the concept of dropwise condensation, Int. J. Heat Mass Transfer 49 (3–4) (2006) 649–657.

[5] R.G.H. Watson, D.C.P. Birt, C.W. Honour, B.W. Ash, The promotion of dropwise condensation by montan wax. I. Heat transfer measurements, Appl. Chem. 12 (1962) 539–546.

[6] R.A. Erb, E. Thelen, Dropwise condensation characteristics of permanent hydrophobic systems, US Department of Interior, Office of Saline Water, R&D Report No. 184, 1966, pp. 54–57.

[7] P.J. Marto, D.J. Looney, J.W. Rose, A.S. Wanniarachchi, Evaluation of organic coatings for the promotion of dropwise condensation of steam, Int. J. Heat Mass Transfer 29 (8) (1986) 1109–1117.

[8] K. Mori, N. Fujita, H. Horie, S. Mori, T. Miyashita, M. Matsuda, Heat transfer promotion of an aluminum–brass cooling tube by surface treatment with triazinethiols, Langmuir 7 (6) (1991) 1161–1166.

[9] G. Koch, K. Kraft, A. Leipertz, Parameter study on the performance of dropwise condensation, Rev. Gén. Therm. 37 (1998) 539–548.

[10] G. Koch, D. Zhang, A. Leipertz, Condensation of steam on the surface of hard coated copper discs, Heat Mass Transfer 32 (1997) 149–156.

[11] G. Koch, D. Zhang, A. Leipertz, Study on plasma enhanced CVD coated material to promote dropwise condensation, Int. J. Heat Mass Transfer 41 (13) (1998) 1899–1906.

[12] A. Leipertz, G. Koch, Dropwise condensation of steam on hard coated surfaces, in: Proceedings of the XIth International Heat Transfer Conference, vol. 6, 1998, pp. 379–384.

[13] D. Zhang, Z. Lin, J. Lin, New surface materials for dropwise condensation, in: Proceedings of the VIIIth International Heat Transfer Conference, vol. 4, 1986, pp. 1677–1682.

[14] Q. Zhao, D. Zhang, S.P. Li, D. Xu, J. Lin, Dropwise condensation of steam on ion-plating surfaces, in: Proceedings of the International Conference on Petroleum Refining and Petrochemical Processing, vol. 2, 1991, pp. 1049–1052.

[15] Q. Zhao, B.M. Burnside, Dropwise condensation of steam on ion implanted condenser surfaces, Heat Recov. Syst. CHP 14 (5) (1994) 525–534.

[16] Q. Zhao, D. Zhang, S.F. Li, D. Xu, G.B. Zhang, J. Lin, New surface materials with dropwise condensation, in: Proceedings of the IVth World Congress of Chemical Engineering, 1991, Sessions 8.3–10.

[17] Q. Zhao, D. Zhang, J. Lin, Surface materials with dropwise condensation made by ion implantation technology, Int. J. Heat Mass Transfer 34 (11) (1991) 2833–2835.

[18] Q. Zhao, D. Zhang, X. Zhu, D. Xu, Z. Lin, J. Lin, Industrial application of dropwise condensation, in: Proceedings of the IXth International Heat Transfer Conference, vol. 4, 1990, pp. 391–394.

[19] A. Leipertz, K.-H. Choi, Dropwise condensation on ion implanted metallic surfaces, in: Proceedings of the Third European Thermal Sciences Conference, 2000, pp. 917–920.

[20] K.-H. Choi, Gezielte Einstellung und wärmetechnische Charakterisierung der Tropfenkondensation auf ionenimplantierten Oberflächen, Dr.-Ing. Thesis, Friedrich-Alexander-University, Erlangen, 2001.

[21] A. Bani Kananeh, M.H. Rausch, A.P. Fröba, A. Leipertz, Experimental study of dropwise condensation on plasma-ion implanted stainless steel tubes, Int. J. Heat Mass Transfer 49 (25,26) (2006) 5018–5026.

[22] T. Young, An essay on the cohesion of fluids, Philos. Trans. R. Soc. London (1805) 65–87.

[23] J. Straub, P. Waas, Tropfenkondensation, in: VDI-Wärmeatlas, VDI-Verlag, Düsseldorf, 1988 (Chapter JC I).

[24] W. Kast, Wärmeübertragung bei Tropfenkondensation, Chem. Ing. Tech. 3 (1963) 163–168.

[25] R.N. Wenzel, Resistance of solid surfaces to wetting by water, Ind. Eng. Chem. 28 (1936) 988–994.

[26] A.W. Neumann, A.H. Abdelmessih, A. Hameed, The role of contact angles and contact angle hysteresis in dropwise condensation heat transfer, Int. J. Heat Mass Transfer 21 (1978) 947–953.

[27] H. Reiss, Warum gibt es Benetzung? Phys. unserer Zeit 23 (5) (1992) 202–212.

[28] Aluminum Standards and Data, The Aluminum Association Inc., 1997.

[29] M. Nastasi, J.W. Mayer, J.K. Hirvonen, Ion–Solid Interactions: Fundamentals and Applications, Cambridge University Press, Cambridge, 1996.

[30] W. Nusselt, Die Oberflächenkondensation des Wasserdampfes, Zeitschrift VDI 60 (27) (1916) 541–546, and 569–575.

[31] H.D. Baehr, K. Stephan, Wärme- und Stoffübertragung, Springer-Verlag, Berlin, 2004.

[32] C.A. Depew, R.L. Reisbig, Vapor condensation on a horizontal tube using teflon to promote dropwise condensation, I&EC Process Des. Develop. 3 (4) (1964) 365–369.

[33] J.W. Rose, Laminar film condensation of pure vapors, in: S.G. Kandlikar, M. Shoji, V.K. Dhir (Eds.), Handbook of Phase Change: Boiling and Condensation, Taylor & Francis, Philadelphia, 1999, pp. 523–536.

[34] K. Stephan, Heat Transfer in Condensation and Boiling, Springer-Verlag, New York, 1992.

[35] http://www.srim.org.

[36] J.W. Rose, Dropwise condensation, in: G.F. Hewitt (Ed.), Heat Exchanger Design Handbook 1998, Begell House, New York, 1998, pp. 2.6.5-1–2.6.5-11.